

Characterization of Zonal Flows and Their Dynamics in Experiment and Simulation

by
C. Holland¹

with
G.R. Tynan¹, J. H Yu¹, A.N. James¹, M. Shimada¹,
D. Nishijima¹, Z. Yan¹, N. Taheri¹, R.J. Fonck²,
G.R. McKee², D. Gupta², J. Candy³, and R.E. Waltz³

¹ University of California, San Diego, CA

² University of Wisconsin-Madison, WI

³ General Atomics, San Diego, CA

Presented at
48th Annual Meeting of the
Division of Plasma Physics
American Physical Society
Philadelphia, Pennsylvania

October 30 – November 3, 2006



Overview of Results

- **Zero mean frequency (ZMF) zonal flow now observed in core of DIII-D**
 - First observation of ZMF in a high-temperature tokamak
 - Transition from ZMF dominated core to Geodesic Acoustic Mode (GAM) dominated edge region documented
- **GAM-Driven Cascade of Internal Energy Has Been Measured in Edge of DIII-D**
 - First direct measurement of zonal flow driven nonlinear energy transfer in a high-temperature tokamak
 - Simulations of core turbulence indicate that ZMF zonal flows drive a similar cascade
- **Generation of a zonal flow via Reynolds stress has been demonstrated in the CSDX experiment at UCSD**
- **Taken together, results represent experimental validation of key linear and nonlinear aspects of the 'drift-wave - zonal flow' paradigm**

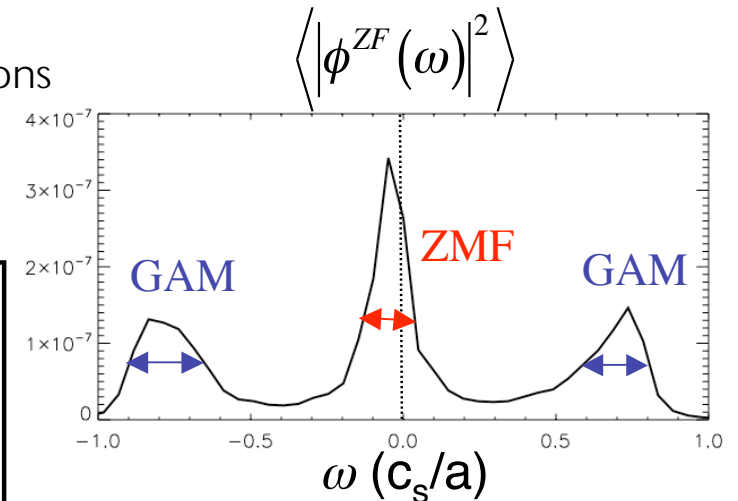
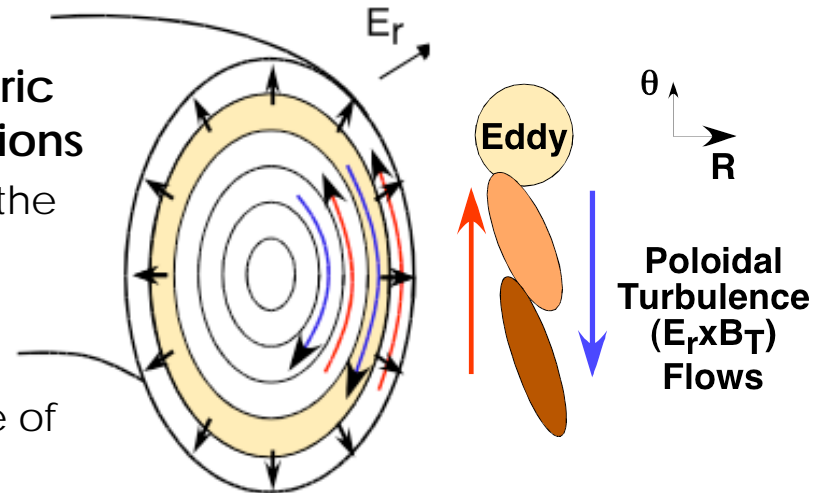
Motivation

- Zonal flows now recognized as essential component for understanding drift-wave turbulence
- They have received extensive analytic and numerical investigation, but experimental results have lagged until recently
 - Experimental observations of the 'zero mean frequency' zonal flow branch as well as nonlinear interactions between turbulence and zonal flows have been extremely limited
- Upgraded Beam Emission Spectroscopy (BES) system on DIII-D now allows for measurement of turbulence and zonal flows over wide region of plasma
- CSDX experiment at UCSD supports complimentary studies of drift-wave turbulence in a basic laboratory experiment
- **Goal:** use BES and CSDX to provide necessary experimental support for theory and simulation of drift-wave - zonal flow turbulence



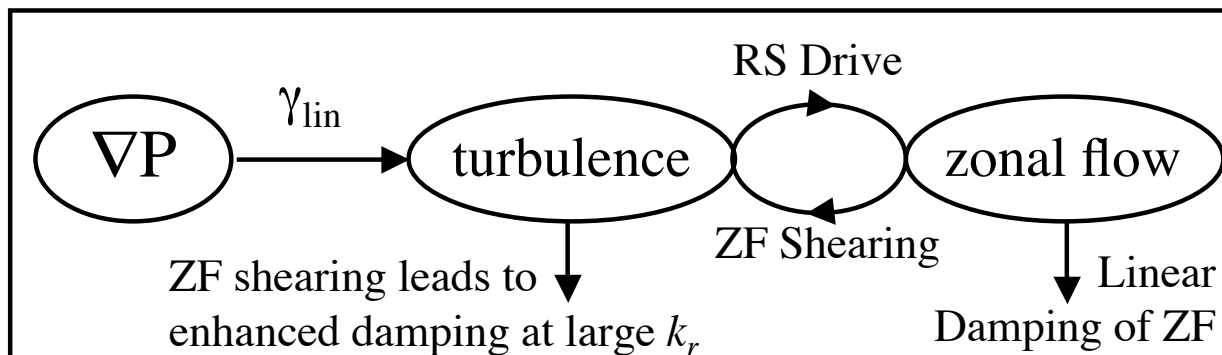
Zonal Flows Believed to Provide Dominant Saturation Mechanism for Drift-Wave Turbulence

- Zonal flows consist of (at minimum) axisymmetric radial electric fields which shear apart fluctuations
 - Nonlinearly generated by the Reynolds stress of the turbulence (Diamond & Kim, PoF B 1991)
- Two branches:
 - a) finite-frequency, rapidly decaying Geodesic Acoustic Mode (GAM); widely observed in edge of many machines
 - b) weakly damped zero mean frequency (ZMF) (Rosenbluth & Hinton, PRL 1998); limited observations (CHS stellerator). Timescale: $\tau_{\text{turb}} < \tau_{\text{ZMF}} < \tau_{\text{equil}}$



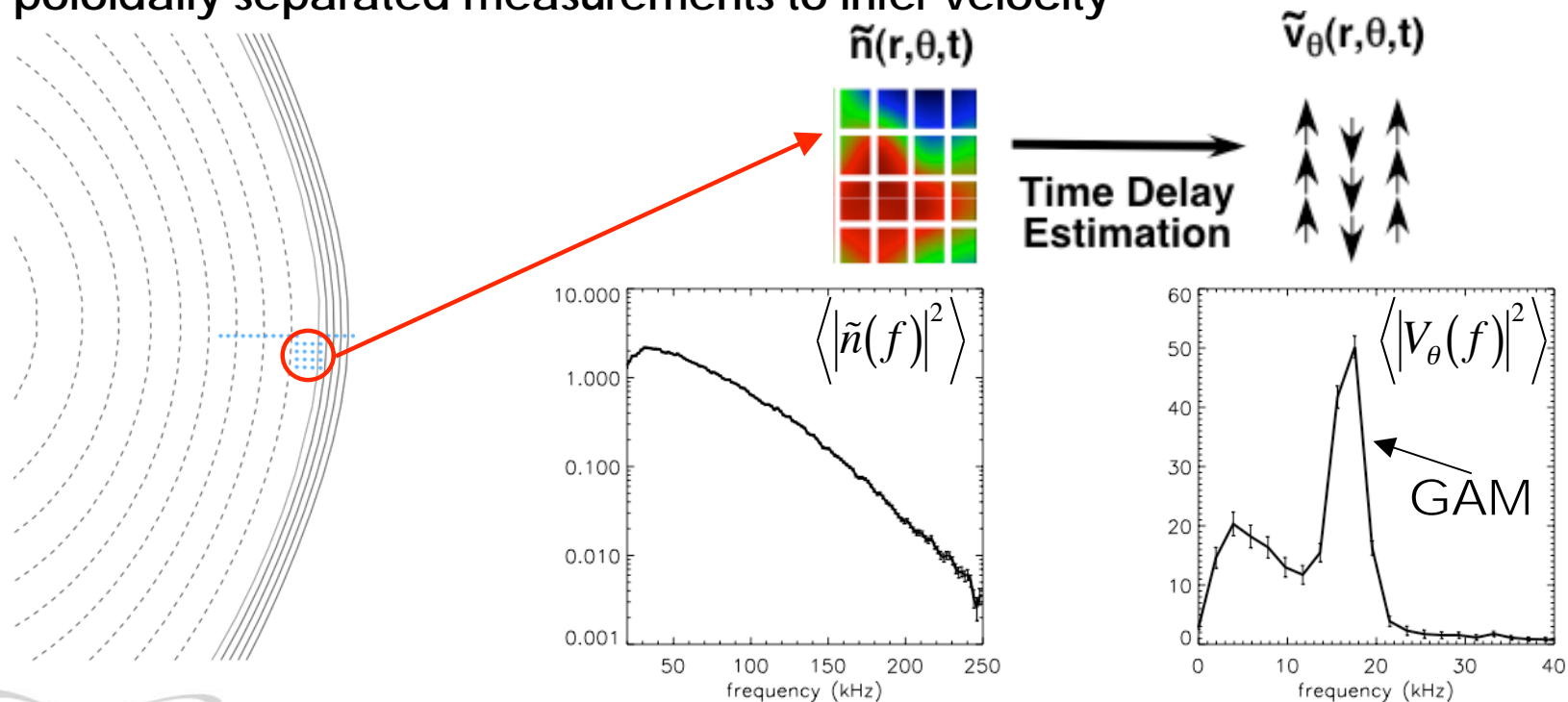
Zonal flow spectrum from GYRO simulation w/ $q = 3$

Drift-Wave - Zonal Flow “Energetics”



BES System Configured to Provide Zonal Flow Measurements Over Large Fraction of Plasma

- BES measures localized, long-wavelength ($k_{\perp}\rho_i < 1$) density fluctuations
 - Can be radially scanned shot to shot to measure turbulence profiles
 - Recent upgrades allow for BES to measure core fluctuations (Gupta *et al*, Rev. Sci. Inst **75** 3493 2004)
- Time-delay estimation (TDE) technique uses cross-correlations between two poloidally separated measurements to infer velocity

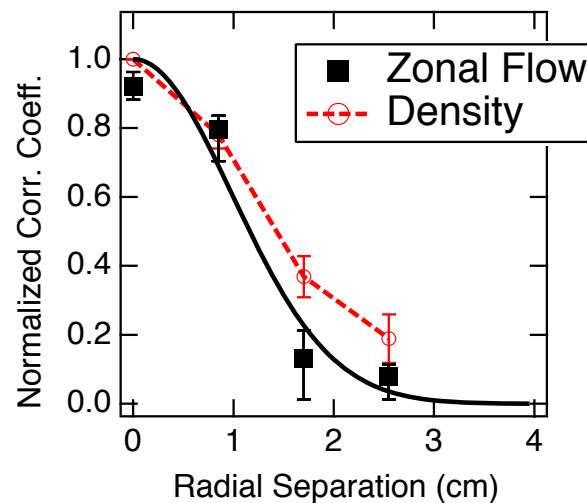


Measured V_θ Spectra Exhibit Signatures of Both ZMF Zonal Flows and GAMs

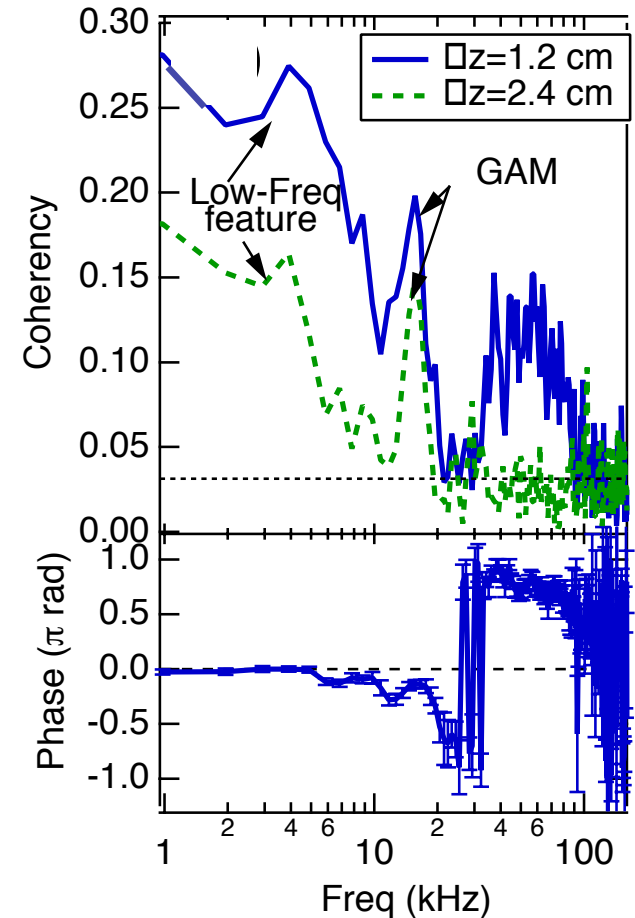
- Spectra indicate broad, low-frequency structure with zero measurable poloidal phase shift
 - Consistent with low- m ($m=0$?)
 - Peaks at/near zero frequency

- GAM also clearly observed near 15 kHz

- ZMF zonal flow has radial correlation length comparable to underlying density fluctuations
 - Necessary for effective shearing of turbulence



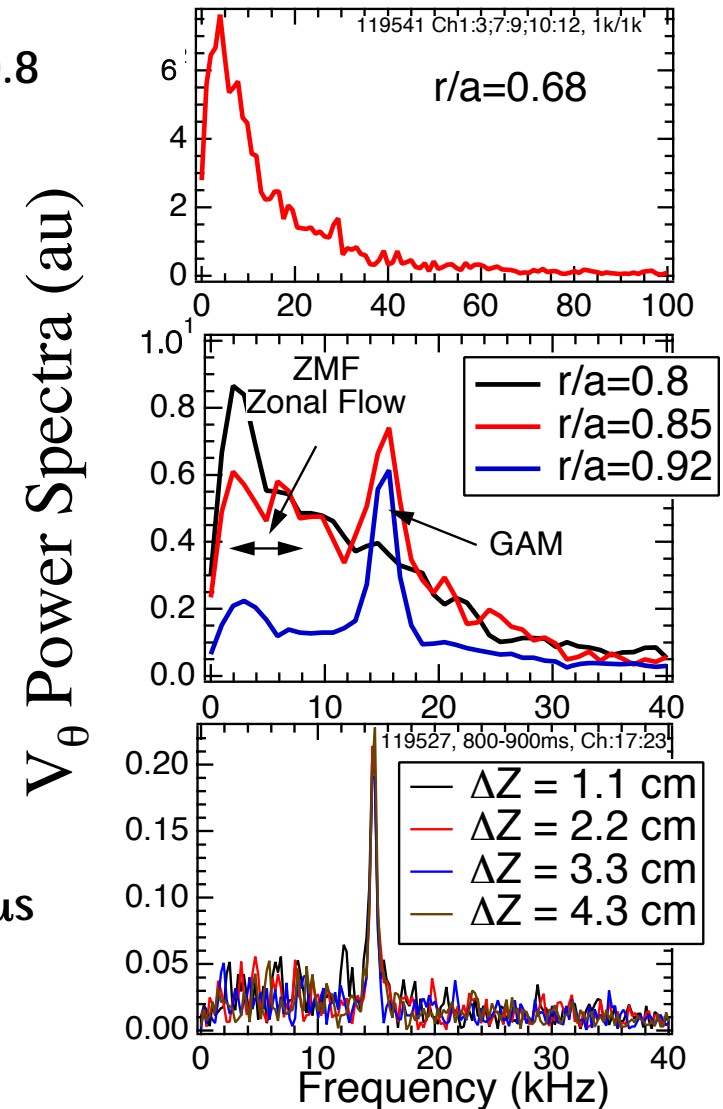
V_θ spectra at $r/a = 0.8$



Gupta *et al.*, PRL **97**
125002 (2006)

Observe Transition from ZMF-Dominated Core to GAM-Dominated Edge

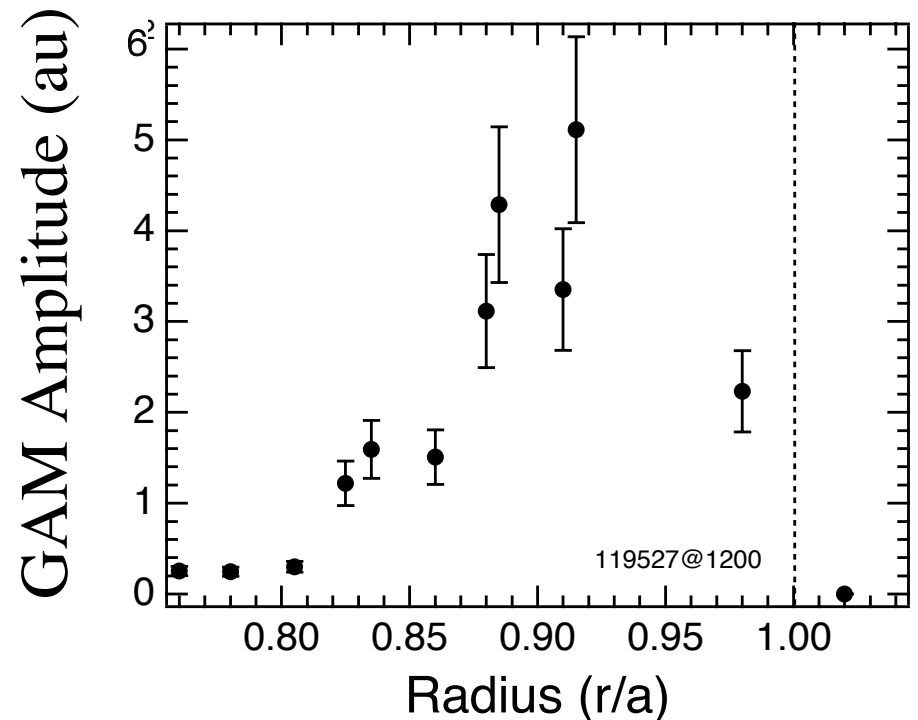
- Velocity spectra show broad ZF spectrum for $r/a < 0.8$
→ ZMF flow
- Superposition of broad spectrum and GAM peak near $r/a = 0.85$
- GAM dominates for $r/a > 0.9$
- Consistent with theory/simulation expectations that GAM strength increases with q
 - Increase in GAM strength with q_{95} also observed (McKee *et al.*, PPCF 2006)
- GAM is highly coherent, with correlation time $\tau_{\text{GAM}} > 1$ ms and oscillation period $1/f_{\text{GAM}} \approx 55 \mu\text{s}$, both larger than turbulence decorrelation time $\tau_{\text{turb}} \sim 10 \mu\text{s}$
 - Indicates GAM is “slow” relative to edge turbulence timescales, and so can effectively interact with turbulence (Hahm *et al.*, PoP '99)



GAMs Observed to Peak in Plasma Edge

- **GAM velocity oscillation amplitude peaks near $r/a \sim 0.9-0.95$**
 - Decays near separatrix
 - Decays inboard, still detectable to $r/a \sim 0.75$
 - Consistent with HIBP measurements on JFT-2M (Ito *et al.*, PPCF 2006)
- **ZMF zonal flows not observed for $r/a > \sim 0.9$, but do increase towards core**
 - Harder to quantify radial dependence because of broad spectral characteristics

GAM Amplitude vs. Minor Radius



McKee *et al.*, PPCF 2006

Measuring Nonlinear Interactions Between Zonal Flows and Turbulence

- **Analytic theory and simulation clearly indicate the importance of specific nonlinear interactions between the zonal flows and underlying drift-wave turbulence**
 - Zonal flows should shear apart the turbulence, transferring energy to smaller (radial) scales
 - Turbulence in turn generates zonal flows via the Reynolds stress
- **Experimental validation of the 'drift-wave - zonal flow' paradigm requires measuring these nonlinear interactions, in addition to characterizing the spatio-temporal characteristics of the zonal flows**
- **Present two measurements that address this issue**
 1. GAM-driven nonlinear energy transfer in edge of DIII-D
 2. Generation of a zonal flow by the Reynolds stress in CSDX

Measuring Nonlinear Energy Transfer in Experiment

- Consider a simple model of density evolution

$$\frac{\partial \tilde{n}}{\partial t} \approx -V_x \frac{dn_0}{dx} - V_x \frac{\partial \tilde{n}}{\partial x} - V_y \frac{\partial \tilde{n}}{\partial y} + D \nabla_{\perp}^2 \tilde{n}$$

$$x = r - r_0$$

$$y = r_0 \theta$$

Measuring Nonlinear Energy Transfer in Experiment

- Consider a simple model of density evolution

$$\begin{aligned}x &= r - r_0 \\ y &= r_0 \theta\end{aligned}$$

$$\begin{aligned}\frac{\partial \tilde{n}}{\partial t} &\approx -V_x \frac{dn_0}{dx} - V_x \frac{\partial \tilde{n}}{\partial x} - V_y \frac{\partial \tilde{n}}{\partial y} + D \nabla_{\perp}^2 \tilde{n} \\ \rightarrow \frac{1}{2} \frac{\partial \langle |\tilde{n}|^2 \rangle}{\partial t} &= -\langle \Gamma_x \rangle \frac{dn_0}{dx} - \text{Re} \left\langle \tilde{n}^* V_x \frac{\partial \tilde{n}}{\partial x} \right\rangle - \text{Re} \left\langle \tilde{n}^* V_y \frac{\partial \tilde{n}}{\partial y} \right\rangle + D \langle |\nabla_{\perp} \tilde{n}|^2 \rangle \\ &= -\langle \Gamma_x(f) \rangle \frac{dn_0}{dx} + \sum_{f'} T_n^X(f, f') + \sum_{f'} T_n^Y(f, f') + D \langle |\nabla_{\perp} \tilde{n}(f)|^2 \rangle\end{aligned}$$

Measuring Nonlinear Energy Transfer in Experiment

- Consider a simple model of density evolution

$$x = r - r_0$$

$$y = r_0 \theta$$

$$\frac{\partial \tilde{n}}{\partial t} \approx -V_x \frac{dn_0}{dx} - V_x \frac{\partial \tilde{n}}{\partial x} - V_y \frac{\partial \tilde{n}}{\partial y} + D \nabla_{\perp}^2 \tilde{n}$$

$$\rightarrow \frac{1}{2} \frac{\partial \langle |\tilde{n}|^2 \rangle}{\partial t} = -\langle \Gamma_x \rangle \frac{dn_0}{dx} - \text{Re} \left\langle \tilde{n}^* V_x \frac{\partial \tilde{n}}{\partial x} \right\rangle - \text{Re} \left\langle \tilde{n}^* V_y \frac{\partial \tilde{n}}{\partial y} \right\rangle + D \langle |\nabla_{\perp} \tilde{n}|^2 \rangle$$

$$= \boxed{-\langle \Gamma_x(f) \rangle \frac{dn_0}{dx}} + \boxed{\sum_{f'} T_n^X(f, f') + \sum_{f'} T_n^Y(f, f')} + \boxed{D \langle |\nabla_{\perp} \tilde{n}(f)|^2 \rangle}$$

Coupling of flux to background density gradient (source)

Nonlinear “three-wave” interactions which exchange energy between different space/timescales

$$T_n^X(f, f') = -\text{Re} \left\langle \tilde{n}^*(f) V_x(f - f') \frac{\partial \tilde{n}}{\partial x}(f') \right\rangle$$

$$T_n^Y(f, f') = -\text{Re} \left\langle \tilde{n}^*(f) V_y(f - f') \frac{\partial \tilde{n}}{\partial y}(f') \right\rangle$$

Collisional dissipation of fluctuation energy (sink)

Measuring Nonlinear Energy Transfer in Experiment

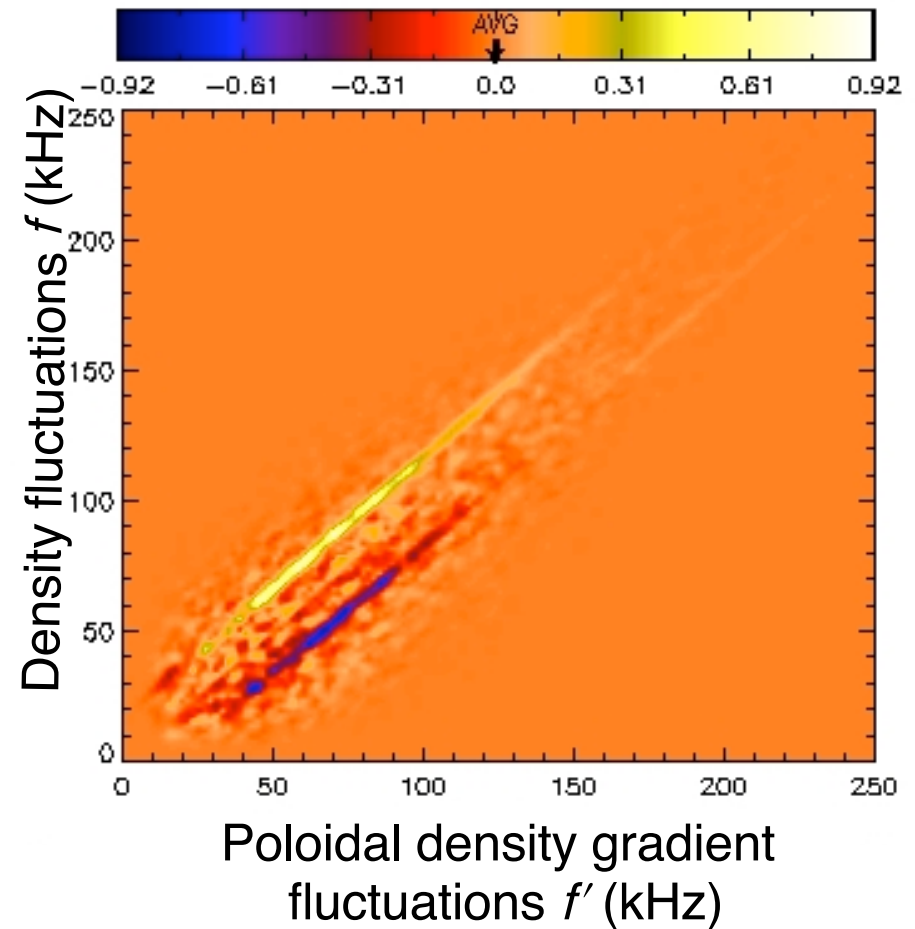
$$T_n^Y(f', f) = -\text{Re} \left\langle n^*(f) V_y(f - f') \frac{\partial n}{\partial y}(f') \right\rangle$$

- $T_n^Y(f', f)$ measures the transfer of energy between density fluctuations at f and poloidal density gradient fluctuations at f' at a specific spatial location due to poloidal convection
 - A **positive value** of T_n^Y indicates that $n(f)$ is **gaining energy** from $\partial n / \partial y(f')$
 - A **negative value** indicates that $n(f)$ is **losing energy** to $\partial n / \partial y(f')$
- Have all the quantities needed to *experimentally* calculate the portion of $T_n^Y(f', f)$ associated with GAM convection (with $\delta I \approx n$)
 1. $n(r, t) = (n_1 + n_2) / 2$
 2. $\partial n / \partial y(r, t) = (n_1 - n_2) / \Delta y$
 3. $V_y(r, t)$ from TDE algorithm

GAMs Drive Clear Forward Cascade of Internal Energy in Frequency Space

- $T_n^Y(f, f)$ clearly shows that fluctuations at $f = f + f_{\text{GAM}}$ gain energy, while those at $f = f - f_{\text{GAM}}$ lose energy

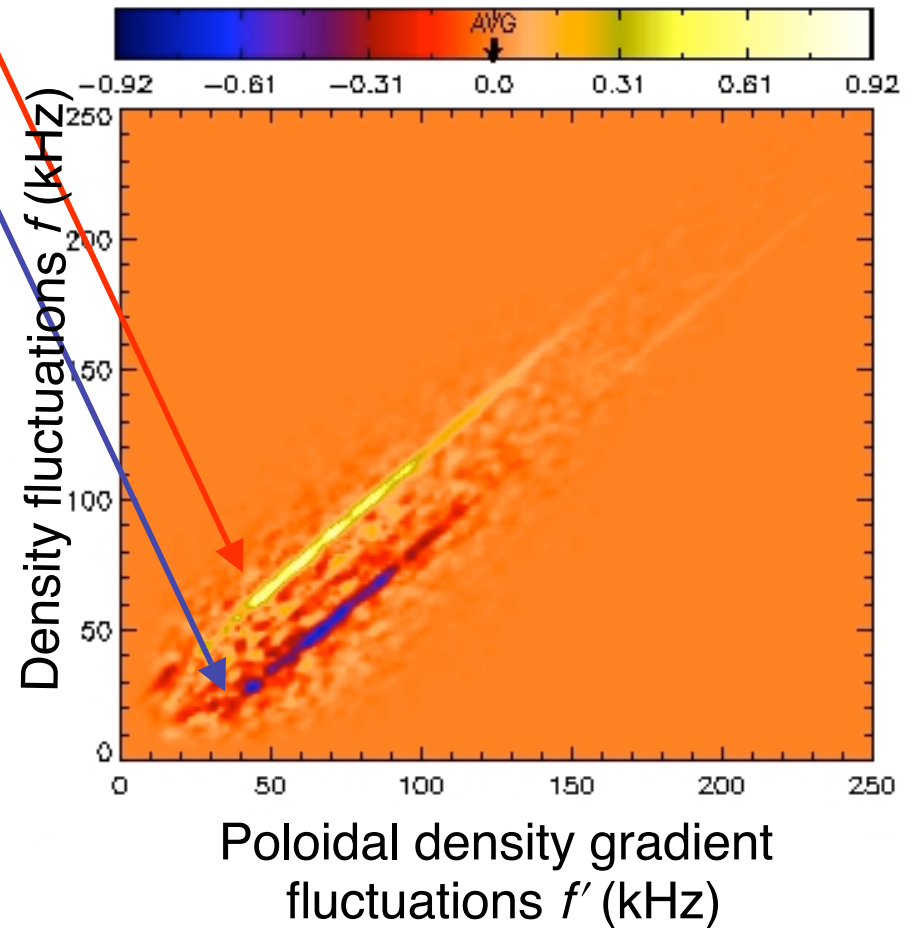
$$T_n^Y(f', f) = -\text{Re} \left\langle \tilde{n}^*(f) V_y(f - f') \frac{\partial \tilde{n}}{\partial y}(f') \right\rangle$$



GAMs Drive Clear Forward Cascade of Internal Energy in Frequency Space

- $T_n^Y(f, f)$ clearly shows that fluctuations at $f = f + f_{\text{GAM}}$ gain energy, while those at $f = f - f_{\text{GAM}}$ lose energy

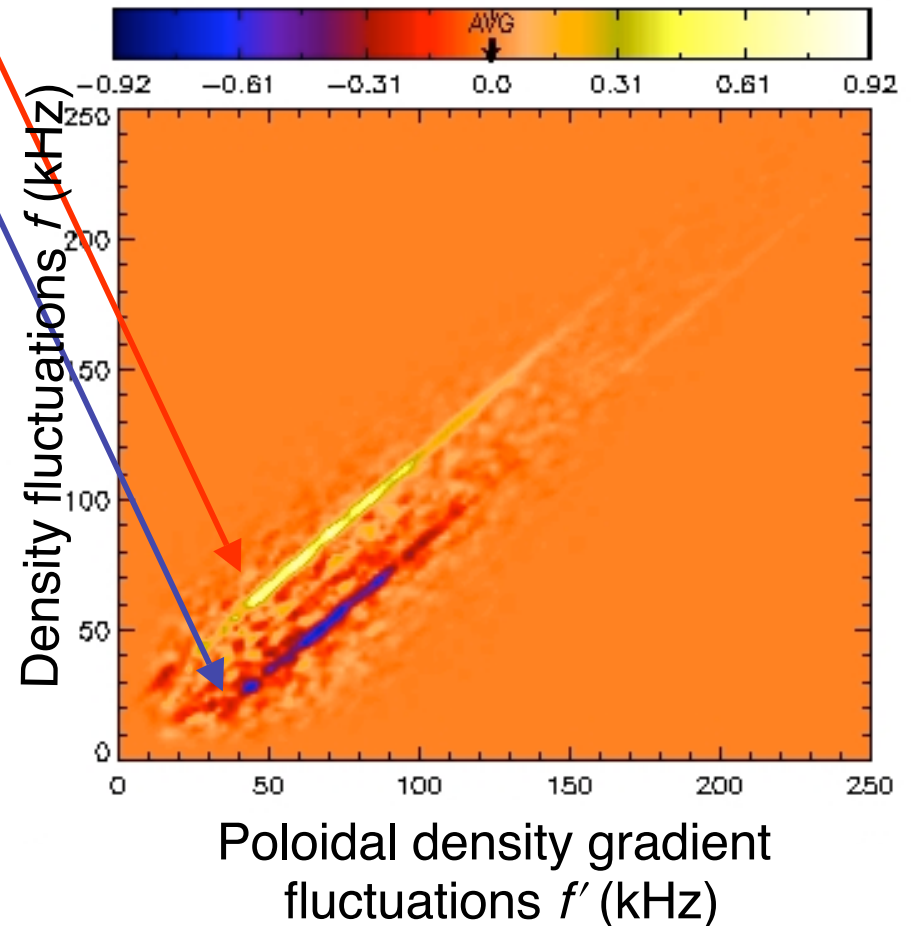
$$T_n^Y(f', f) = -\text{Re} \left\langle \tilde{n}^*(f) V_y(f - f') \frac{\partial \tilde{n}}{\partial y}(f') \right\rangle$$



GAMs Drive Clear Forward Cascade of Internal Energy in Frequency Space

- $T_n^Y(f, f)$ clearly shows that fluctuations at $f = f + f_{\text{GAM}}$ gain energy, while those at $f = f - f_{\text{GAM}}$ lose energy
- Density fluctuations gain energy from lower frequency gradient fluctuations, and lose energy to higher frequency gradient fluctuations

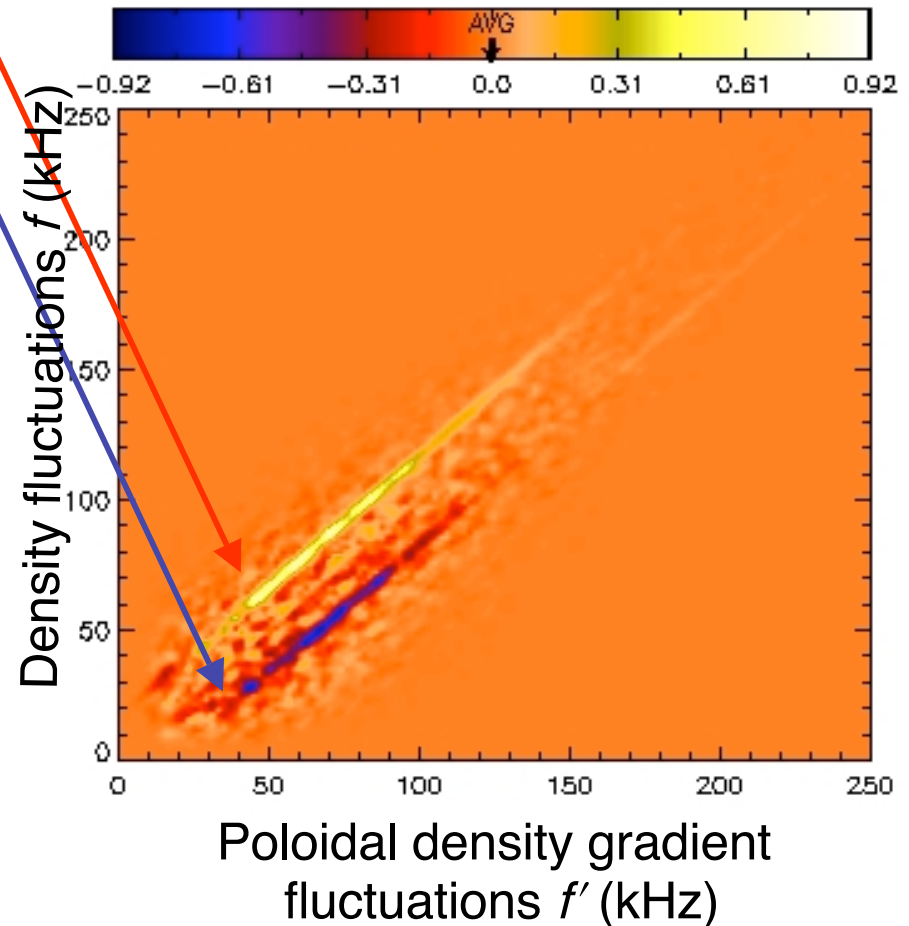
$$T_n^Y(f', f) = -\text{Re} \left\langle \tilde{n}^*(f) V_y(f - f') \frac{\partial \tilde{n}}{\partial y}(f') \right\rangle$$



GAMs Drive Clear Forward Cascade of Internal Energy in Frequency Space

- $T_n^Y(f, f)$ clearly shows that fluctuations at $f = f' + f_{\text{GAM}}$ gain energy, while those at $f = f' - f_{\text{GAM}}$ lose energy
 - Density fluctuations gain energy from lower frequency gradient fluctuations, and lose energy to higher frequency gradient fluctuations
 - Simple picture: energy moves between n , $\partial n / \partial y$ to high f in "steps" of f_{GAM}
- net transfer of energy to high f !

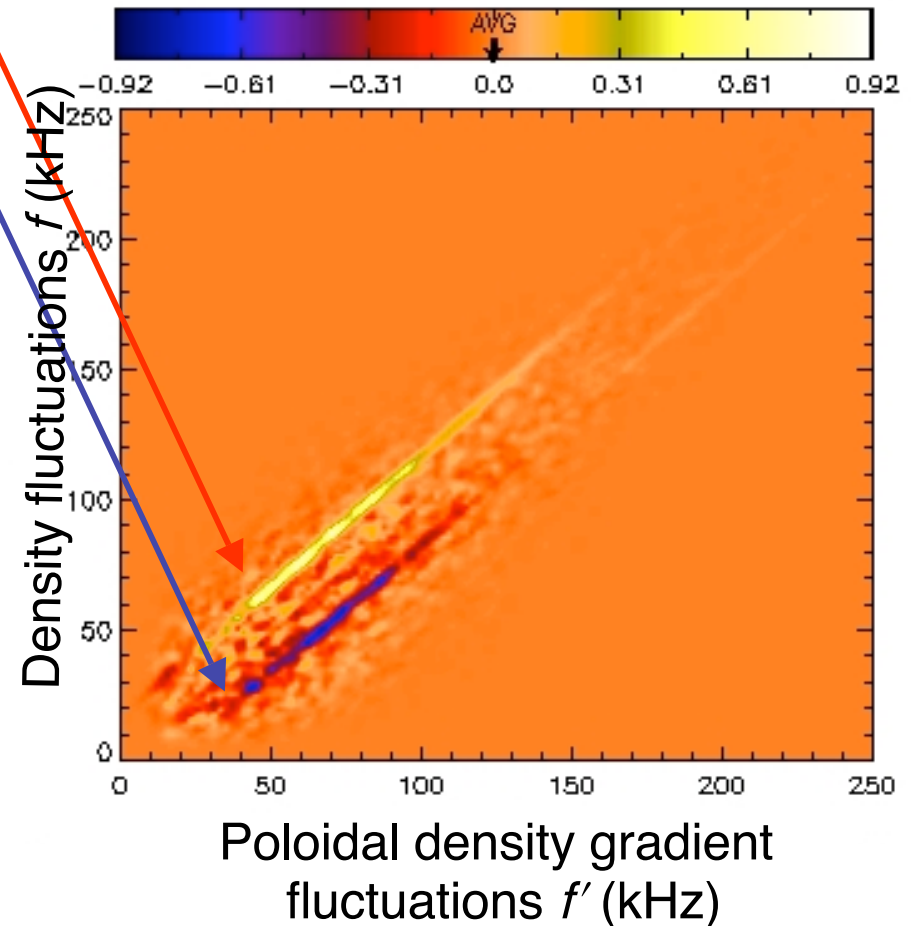
$$T_n^Y(f', f) = -\text{Re} \left\langle \tilde{n}^*(f) V_y(f - f') \frac{\partial \tilde{n}}{\partial y}(f') \right\rangle$$



GAMs Drive Clear Forward Cascade of Internal Energy in Frequency Space

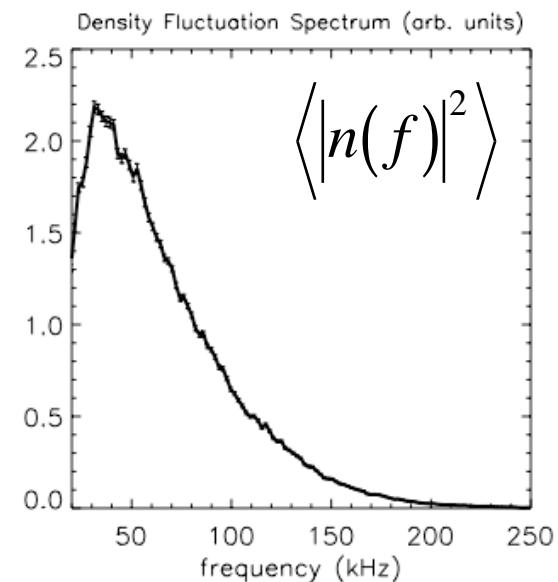
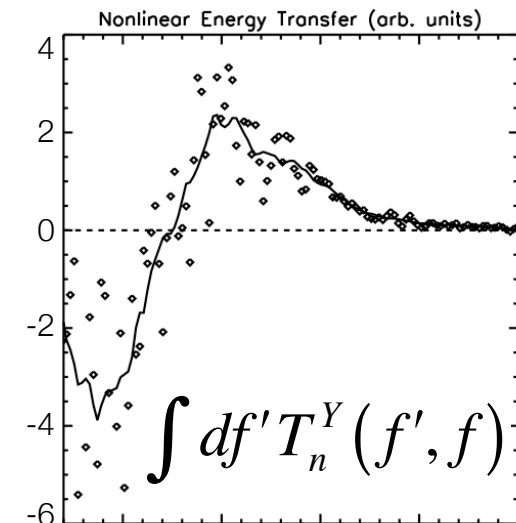
- $T_n^Y(f, f)$ clearly shows that fluctuations at $f = f' + f_{\text{GAM}}$ gain energy, while those at $f = f' - f_{\text{GAM}}$ lose energy
- Density fluctuations gain energy from lower frequency gradient fluctuations, and lose energy to higher frequency gradient fluctuations
- Simple picture: energy moves between n , $\partial n / \partial y$ to high f in "steps" of f_{GAM}
- net transfer of energy to high f !
- Demonstrates that the convection of density fluctuations by the GAM leads to a cascade of internal energy to high f

$$T_n^Y(f', f) = -\text{Re} \left\langle \tilde{n}^*(f) V_y(f - f') \frac{\partial \tilde{n}}{\partial y}(f') \right\rangle$$



GAM Convection Leads to Net Energy Transfer From Low to High Frequencies

- Integrating $T_n^Y(f', f)$ over f' quantifies net rate at which poloidal convection nonlinear transfers energy into / out of fluctuations with frequency f
- Balances linear growth / damping *and* nonlinear transfer due to radial convection to determine turbulent spectrum
- **Key question:** how to clearly connect to shearing mechanism?
 - **First step:** investigate frequency and wavenumber space transfer in simulation

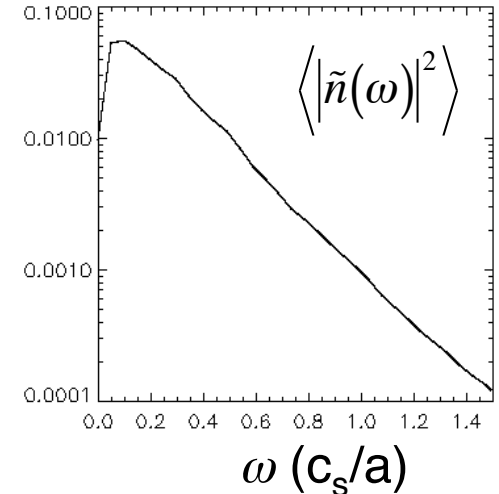
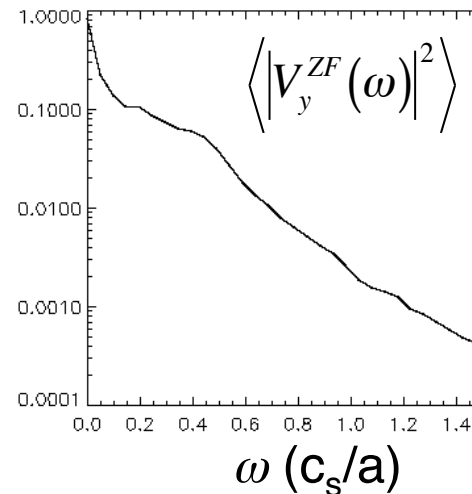
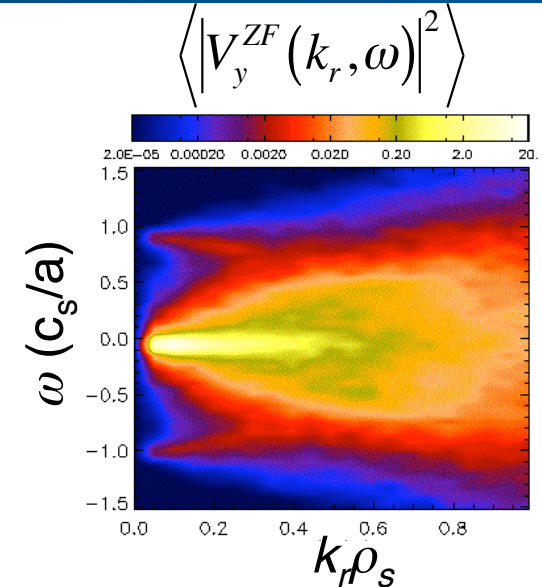
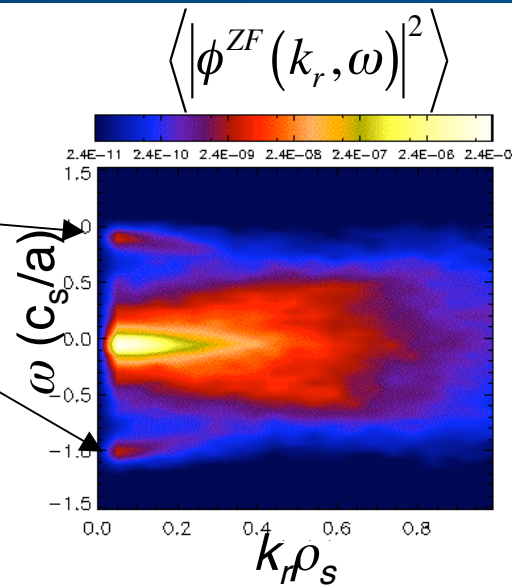


Studying Energy Transfer in Simulation

- To gain more insight into zonal flows driven energy transfer, use the GYRO code to look at the interactions in more detail
- Use CYCLONE base case parameters ($q = 1.4$, $r \frac{d(\ln q)}{dr} = 0.786$, $R/L_n = 2.22$, $R/L_T = 6.92$, $T_e/T_i = 1$)
 - Assumes adiabatic electrons: $\tilde{n}/n_0 = e(\phi - \langle \phi \rangle)/T_e$
 - All analysis is done at outboard midplane
 - Long run time ($T = 3000 a/C_s$) needed for converged statistics
 - Corresponds to core rather than edge turbulence parameters
- Goal is to examine energy transfer in a simple, well-studied model of the turbulence rather than quantitative reproduction of the experimental results
 - CYCLONE parameters represent logical point for this study

Simulation Exhibits Broad Density Spectrum and ZMF Dominated Zonal Flows

- For $q = 1.4$ (and adiabatic electrons), GAMs are weak feature at $\omega \sim \pm c_s/a$ and low k_r
- Zonal flow ExB velocity $cE_r/B \propto k_r \phi$, such that GAM contribution to velocity is overwhelmed by higher k_r components
- Density spectrum broad and featureless



Connecting to Wavenumber-Space Energy Transfer

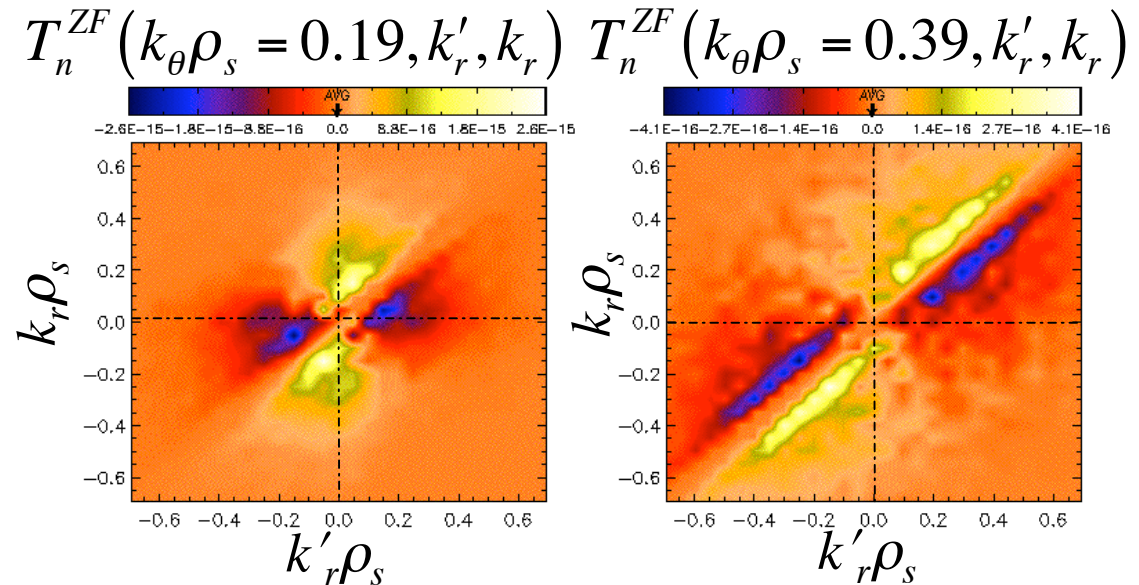
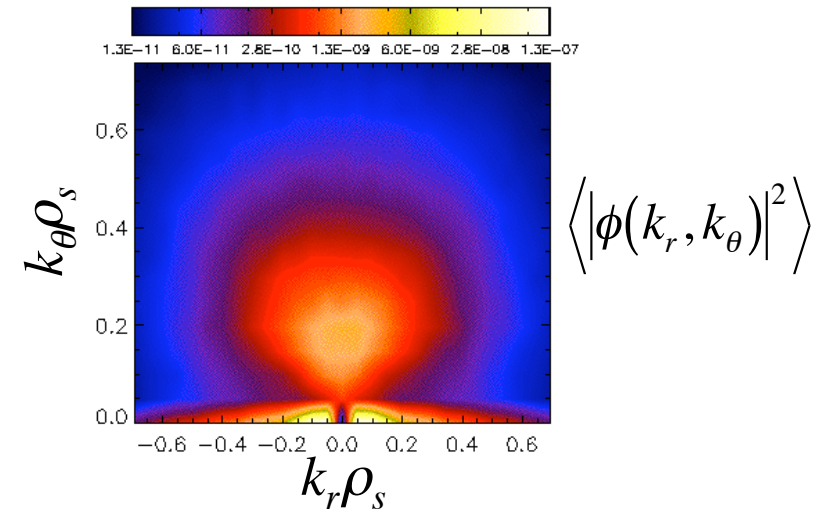
- Experimental results showed a forward cascade in frequency space at a particular spatial location, but would like to make more direct contact with theory which describes transfer between different wavenumbers
- To quantify effects of zonal flow convection on internal energy transfer in GYRO, look at k -space resolved energy transfer term $T_n^{ZF}(k_\theta, k_r, k_r')$

$$T_n^{ZF}(k_\theta, k_r, k_r') = -\text{Re}\langle \tilde{n}^* \vec{V}_{ZF} \cdot \vec{\nabla} \tilde{n} \rangle$$
$$\rightarrow T_n^{ZF}(k_\theta, k_r, k_r') = k_\theta (k_r - k_r') \text{Re}\langle \tilde{n}^*(k_r, k_\theta) \phi(k_r - k_r', k_\theta = 0) \tilde{n}(k_r', k_\theta) \rangle$$

- Note that because zonal flows have $k_\theta = 0$, they couple density fluctuations with different values of k_r , but the same k_θ
 - Can either sum over k_θ , or select specific values of k_θ to gain insight into how zonal flows affect turbulence on different spatial scales

k -space Energy Transfer Shows Forward Cascade In $|k_r|$, In Agreement with Expectations From Theory

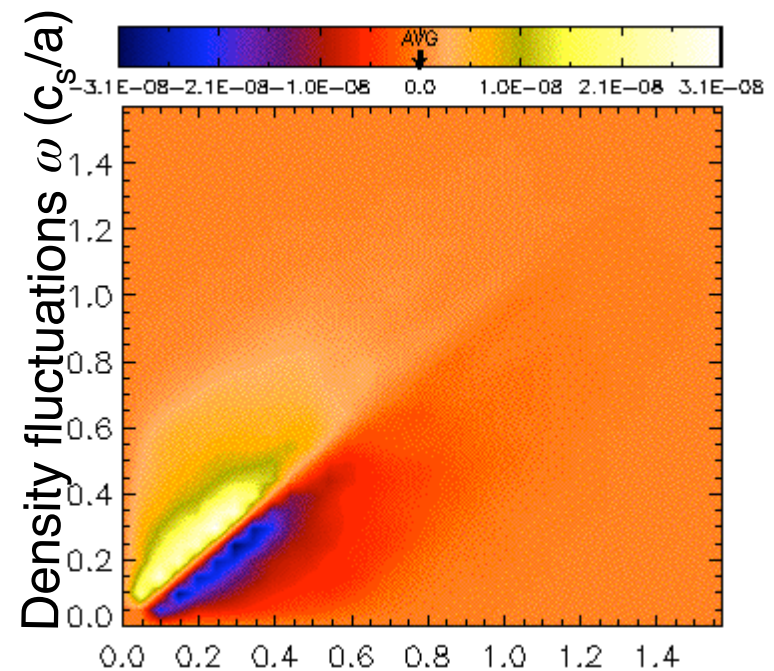
- Fluctuations with $|k_r| > |k_r'|$ gaining energy, while those with $|k_r| < |k_r'|$ losing energy
- Corresponds to expectation that radial decorrelation by ZFs leads to transfer of energy to smaller radial scales (higher k_r)
- So what does frequency-space transfer look like?



ZMF Zonal Flows Also Drive Forward Cascade in Frequency Space

- Calculation of $T_n^Y(\omega', \omega)$ in GYRO indicates the ZMF zonal flows transfer internal energy to higher frequencies
- Key difference from experiment: **transfer now occurs in bands along $\omega = \omega'$ with width set by ZF spectral width, rather than along narrow curves $f = f' \pm f_{GAM}$**
- Again, underlying physics picture similar in simulation and experiment, when spectral differences between ZMF modes and GAMs are accounted for

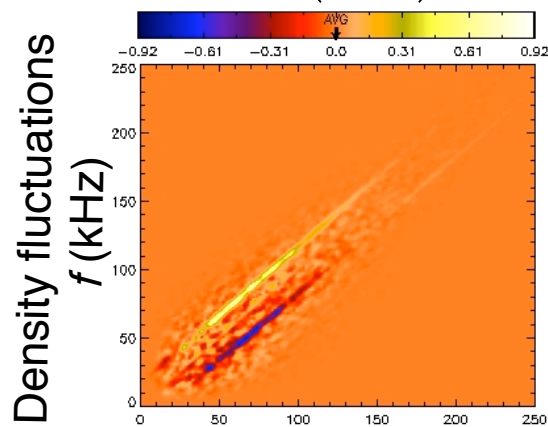
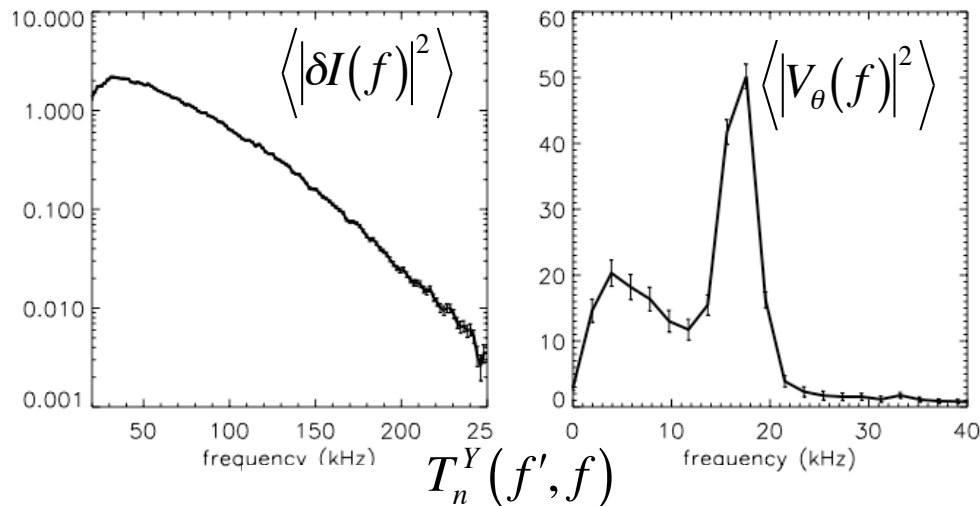
$$T_n^Y(\omega', \omega) = -\text{Re} \left\langle \tilde{n}^*(\omega) V_y^{ZF}(\omega - \omega') \frac{\partial \tilde{n}}{\partial y}(\omega') \right\rangle$$



Poloidal density gradient fluctuations ω' (c_s/a)

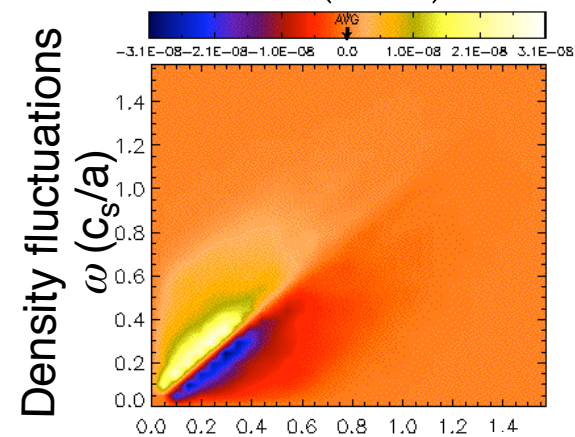
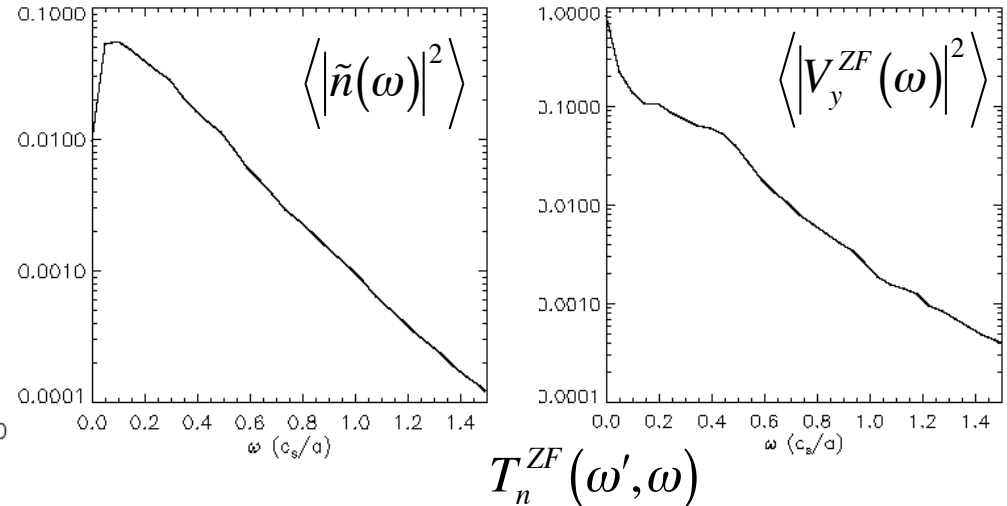
Comparison of Experimental and Simulation Energy Transfer Results Illustrates Similarities

DIII-D edge



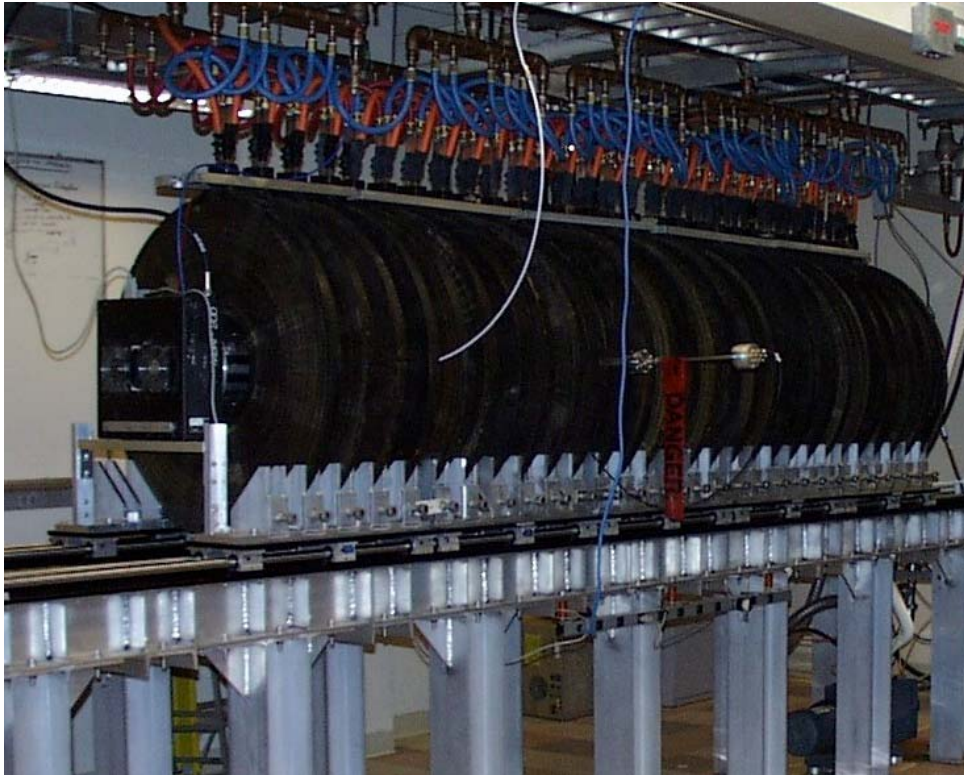
Poloidal density gradient fluctuations f' (kHz)

GYRO



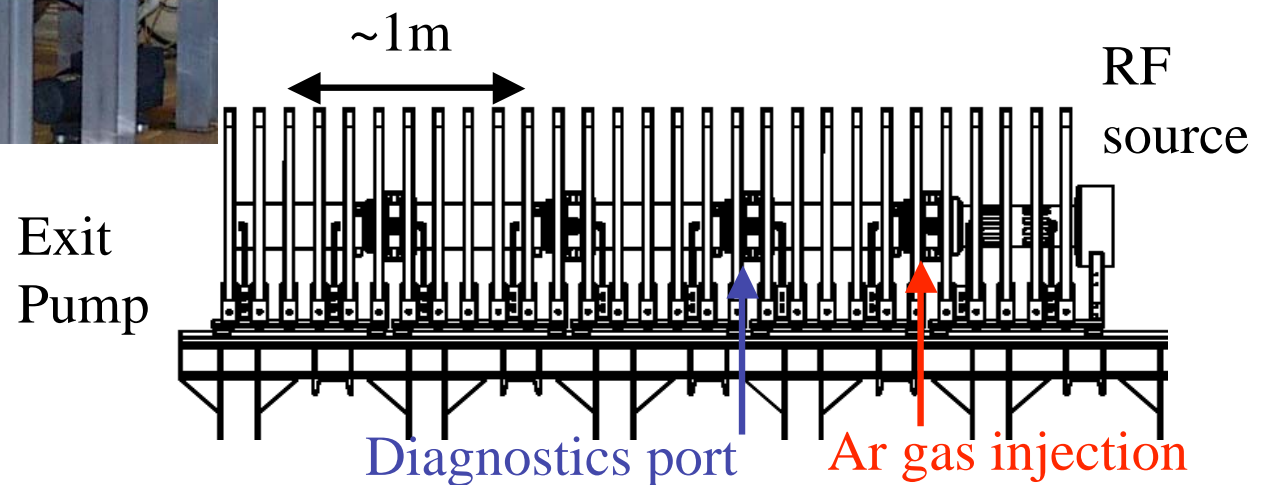
Poloidal density gradient fluctuations ω' (c_s/a)

Controlled Shear Decorrelation Experiment (CSDX) at the University of California, San Diego



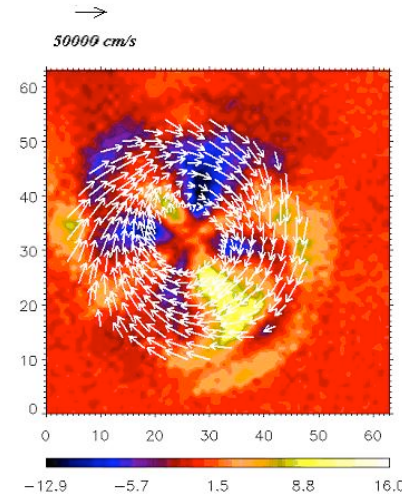
CSDX Parameters

- Helicon source ($m = 0$, 1.5 kW, 13.5 MHz)
- $n_e = 10^{13} \text{ cm}^{-3}$
- $T_e = 3 \text{ eV}$, $T_i \sim 1 \text{ eV}$
- $B = 980 \text{ G}$

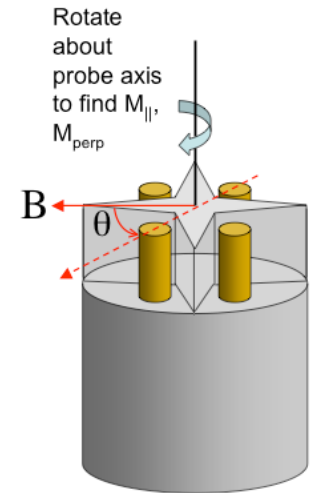


Measuring Zonal Flow Generation in CSDX

- Work at DIII-D focused characterizing zonal flows and how they impact the turbulence
- Complimentary work on CSDX at UCSD on measuring how drift-wave turbulence generates zonal flows via the Reynolds stress
- Multiple diagnostics on CSDX allow us to measure zonal flow velocity and Reynolds stress across machine radius
 - Turbulence clearly identified as collisional drift-waves
- **Plan:** Demonstrate that experimentally measured flow profile consistent with flow expected from azimuthal momentum balance, given the measured Reynolds stress and reasonable damping profiles

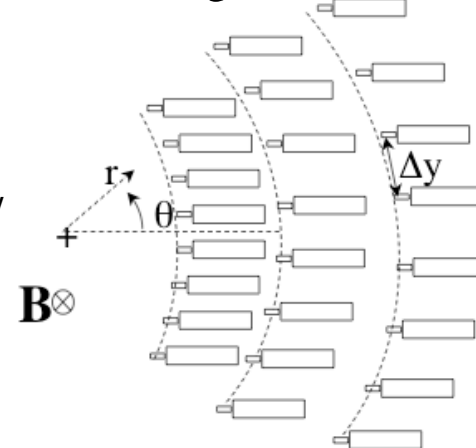


Fast-Framing Camera

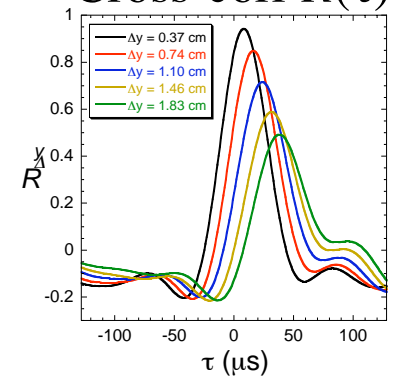


Mach Probe

Langmuir Probe array

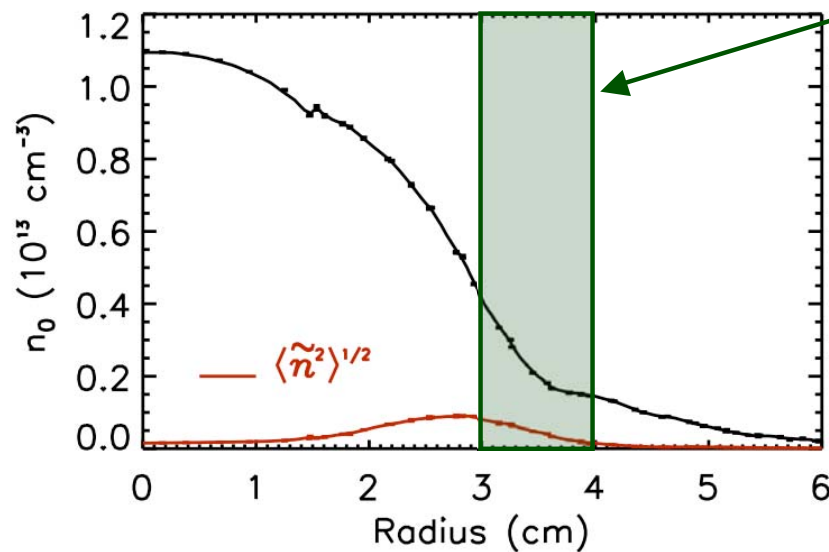
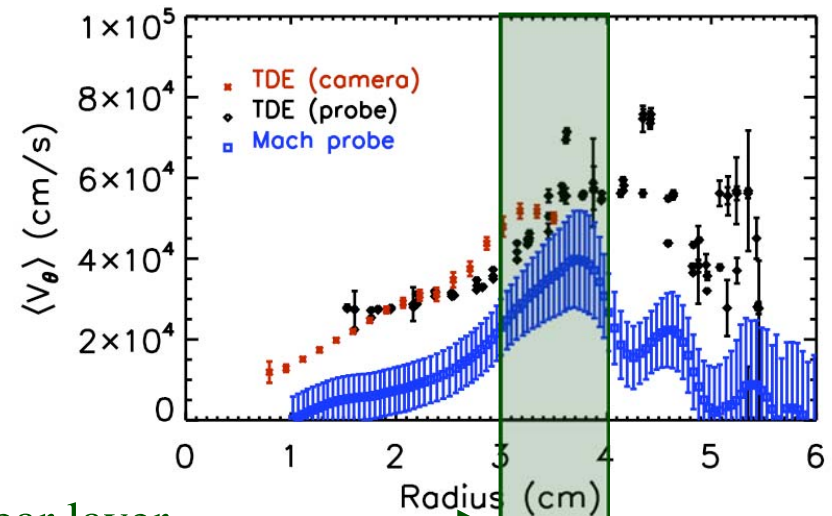


Cross-corr $R(\tau)$

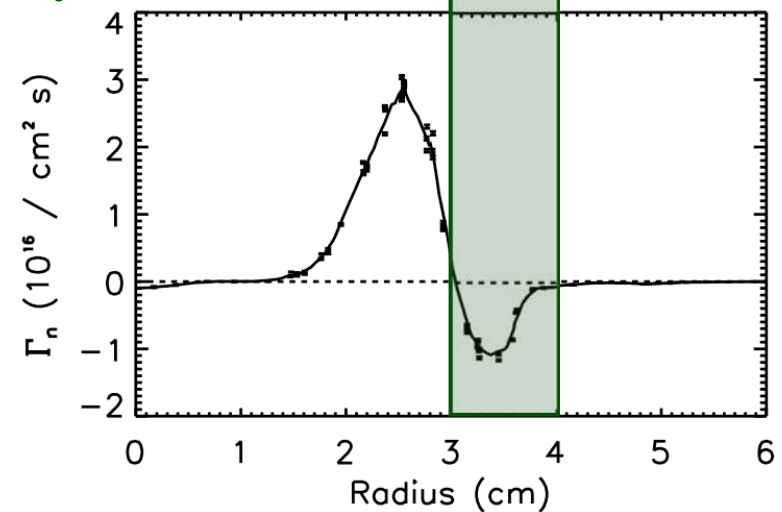


Shear Flow and Associated Flux Suppression Observed in CSDX

- Shear layer at $r \sim 3.5$ cm; particle flux suppressed at this location
- Discrepancy between TDE and Mach probe due to measurement of different quantities (V_{phase} vs. V_i), and intermittent fluctuations at $r > 4$ cm

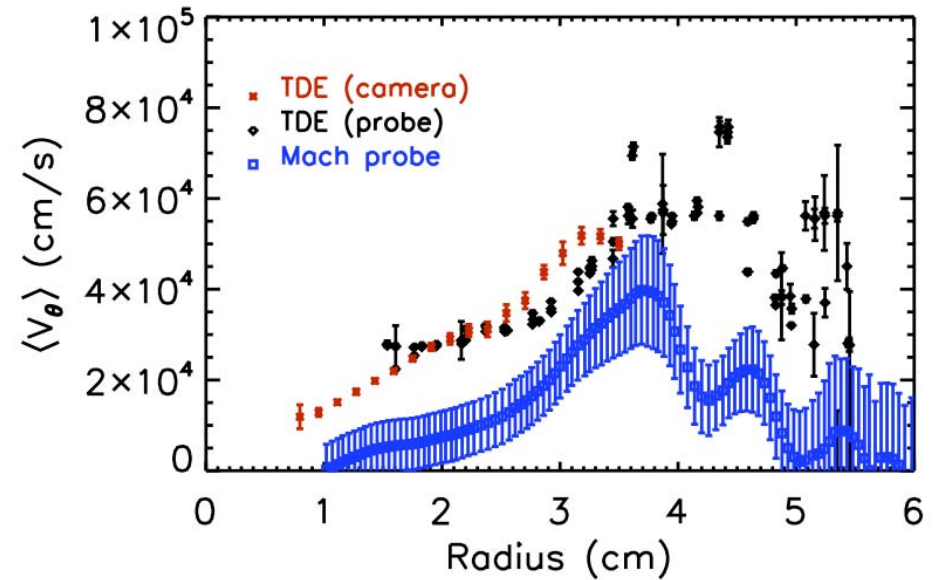


Shear layer →



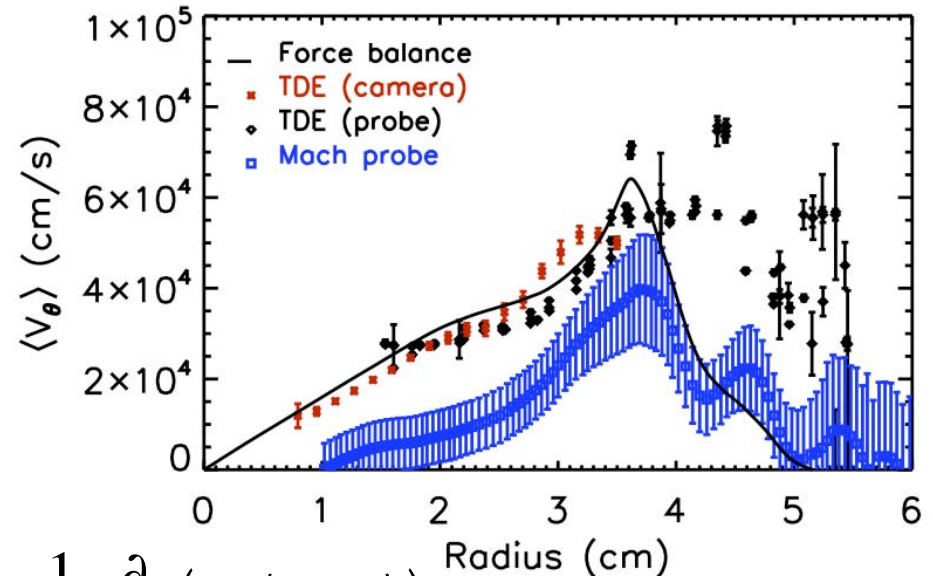
Flow Profile Predicted by Force Balance Consistent With Measured Profile

- Observe sheared mean azimuthal flow profile in CSDX with all diagnostics
 - Shear layer at $r \sim 3.5$ cm; particle flux suppressed at this location

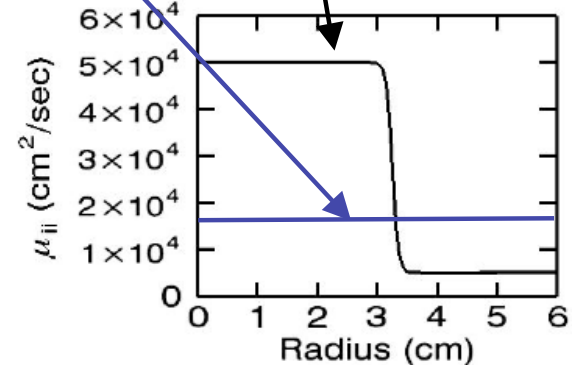
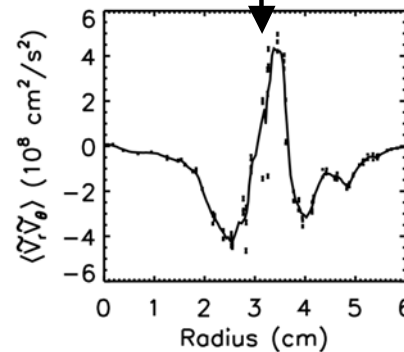


Flow Profile Predicted by Force Balance Consistent With Measured Profile

- Observe sheared mean azimuthal flow profile in CSDX with all diagnostics
 - Shear layer at $r \sim 3.5$ cm; particle flux suppressed at this location
- Measure Reynolds stress using 4-pt Langmuir probe, and integrate force balance equation
 - Prediction in good agreement with measurements
 - Use reasonable guesses for v_{i-n} and μ_{ij} since radially resolved neutral and ion temperature measurements not available

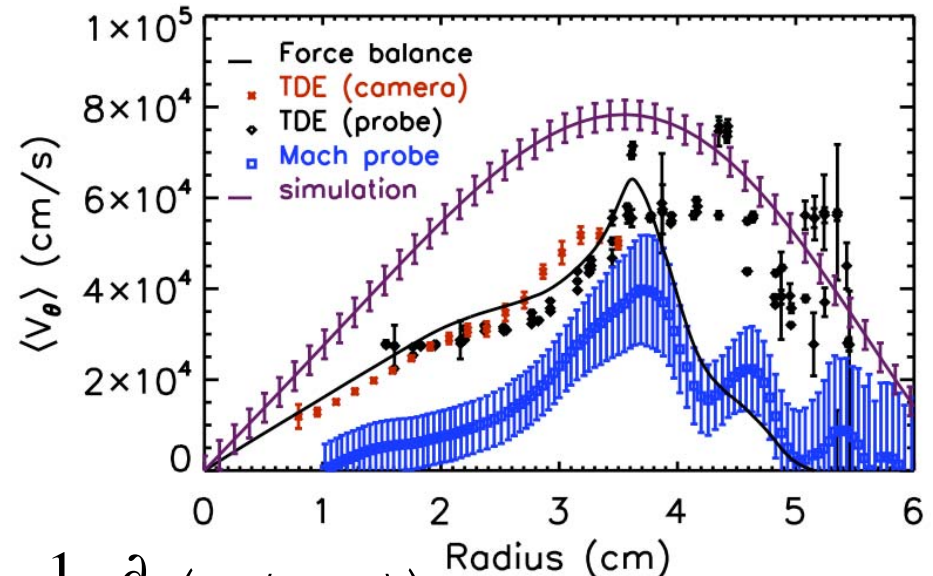


$$\frac{1}{r^2} \frac{\partial}{\partial r} \left(r^2 \langle \tilde{V}_r \tilde{V}_\theta \rangle \right) = -v_{i-n} \langle V_\theta \rangle + \mu_{ii} \nabla^2 \langle V_\theta \rangle$$

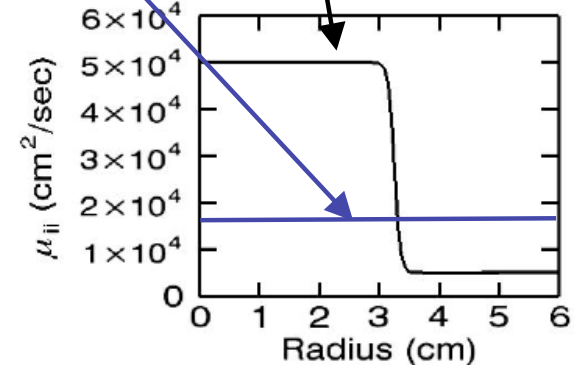
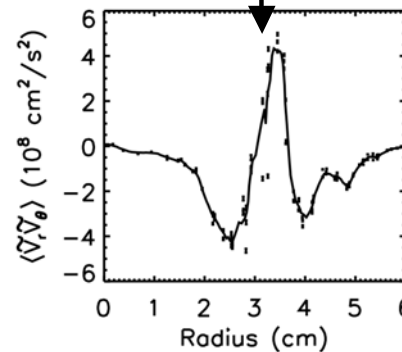


Flow Profile Predicted by Force Balance Consistent With Measured Profile

- Observe sheared mean azimuthal flow profile in CSDX with all diagnostics
 - Shear layer at $r \sim 3.5$ cm; particle flux suppressed at this location
- Measure Reynolds stress using 4-pt Langmuir probe, and integrate force balance equation
 - Prediction in good agreement with measurements
 - Use reasonable guesses for v_{i-n} and μ_{ij} since radially resolved neutral and ion temperature measurements not available
- Simple simulation of collisional drift-waves in CSDX geometry in qualitative agreement
 - Used Hasegawa-Wakatani model



$$\frac{1}{r^2} \frac{\partial}{\partial r} \left(r^2 \langle \tilde{V}_r \tilde{V}_\theta \rangle \right) = -v_{i-n} \langle V_\theta \rangle + \mu_{ii} \nabla^2 \langle V_\theta \rangle$$



Summary of Results

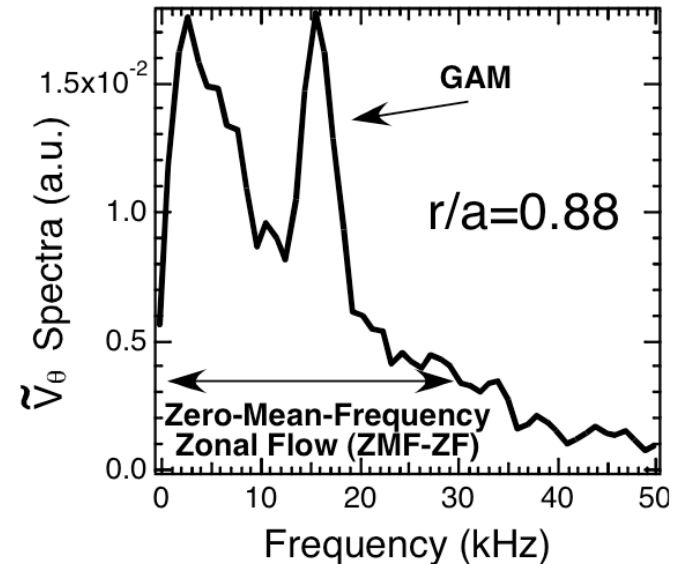
- **Zero mean frequency (ZMF) zonal flow now observed in core of DIII-D**
 - First observation of ZMF in a high-temperature tokamak
 - Transition from ZMF dominated core ($r/a < 0.8$) to Geodesic Acoustic Mode (GAM) dominated edge ($r/a > 0.8$) region documented
- **GAM-Driven Cascade of Internal Energy Has Been Measured in Edge of DIII-D**
 - First direct measurement of zonal flow driven nonlinear energy transfer in a high-temperature tokamak
 - Simulations of core turbulence indicate that ZMF zonal flows drive a similar cascade
- **Generation of a zonal flow via Reynolds stress has been demonstrated in the CSDX experiment at UCSD**
- **Taken together, results represent experimental validation of key linear and nonlinear aspects of the 'drift-wave - zonal flow' paradigm**

Backup slides



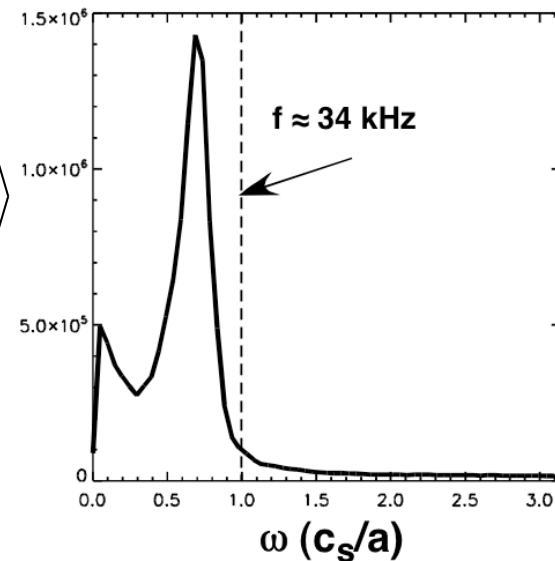
Experimentally Measured Spectra Qualitatively Consistent with Gyrokinetic Simulation

- Measured velocity spectra at $r/a = 0.88$ (top), zonal flow velocity spectrum from GYRO (bottom)
- Simulation used CYCLONE parameters, except $q = 3$ and kinetic electrons
 - $R/L_n = 2.22, R/L_T = 6.92,$
 $T_e/T_i = 1$



$$\langle |V_y^{ZF}(\omega)|^2 \rangle$$

(a.u.)



Good Agreement Between Experiment and Simulation Bicoherence and Biphasé as Well

Express $T_n^Y(f', f)$ in terms of a cross-bicoherence $b(f', f)$ and cross-biphase $\Theta(f', f)$

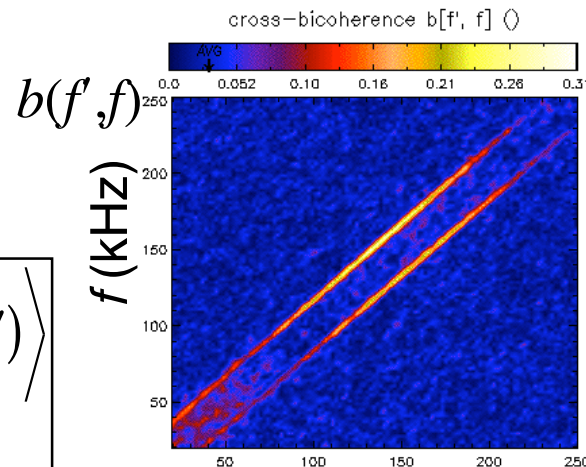
$$T_n^Y(f', f) = -\text{Re} \left\langle \tilde{n}^*(f) V_y(f - f') \frac{\partial \tilde{n}}{\partial y}(f') \right\rangle$$

$$= b(f', f) \cos(\Theta(f', f)) \times$$

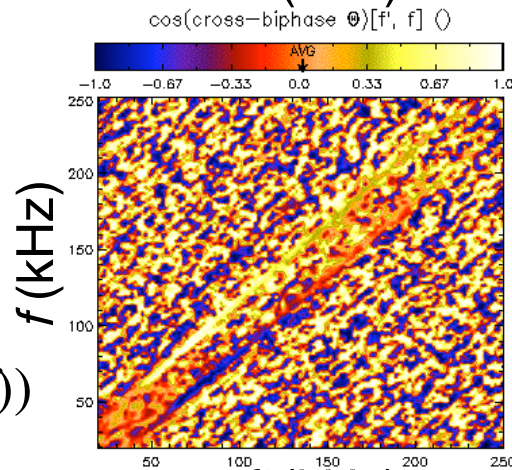
$$\sqrt{\langle |\tilde{n}(f)|^2 \rangle} \sqrt{\left\langle \left| V_y(f - f') \frac{\partial \tilde{n}}{\partial y}(f') \right|^2 \right\rangle}$$

$\cos(\Theta(f', f))$

DIII-D BES

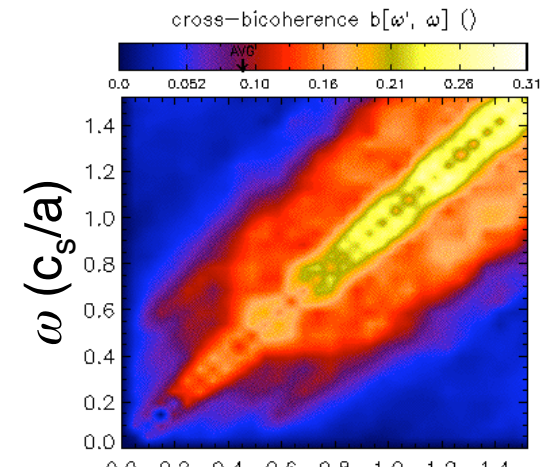


f' (kHz)

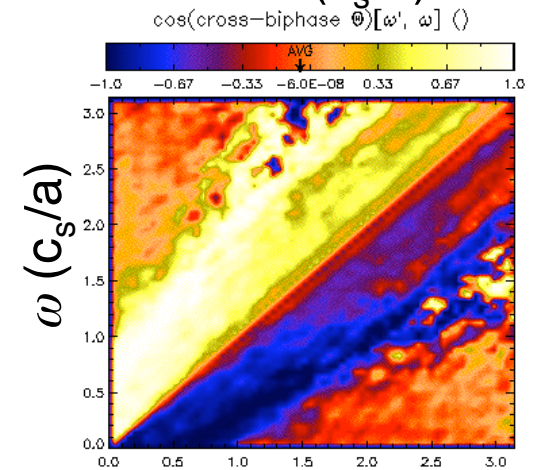


f' (kHz)

GYRO



ω' (c_s/a)



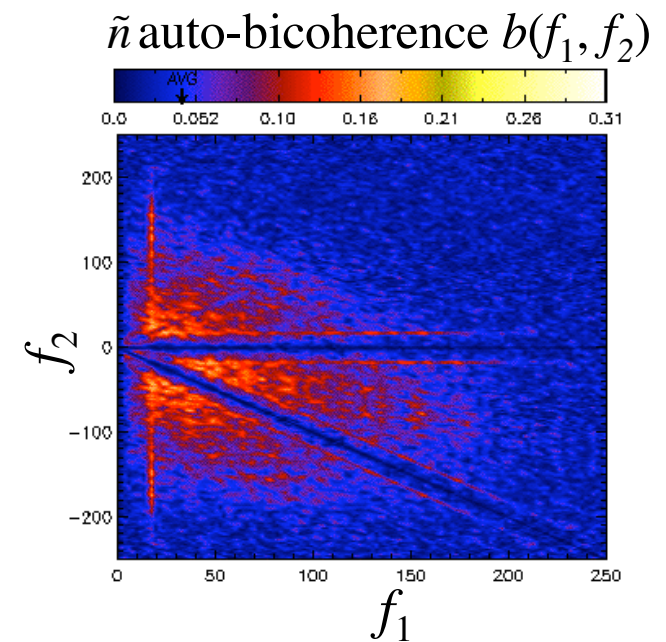
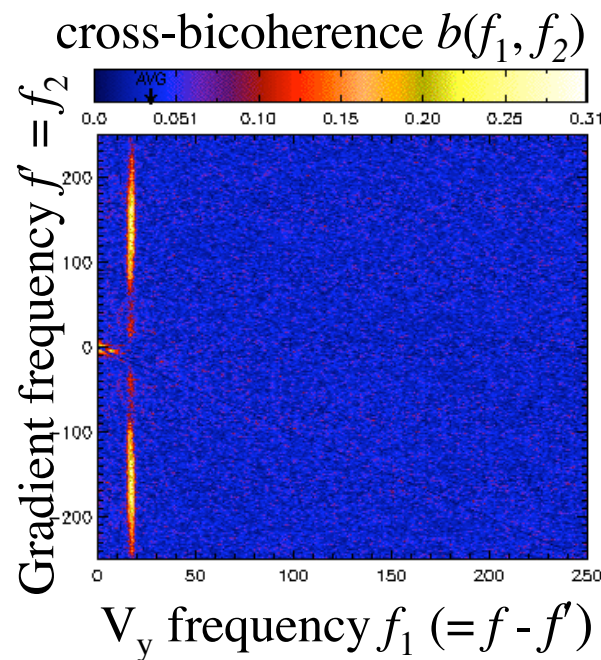
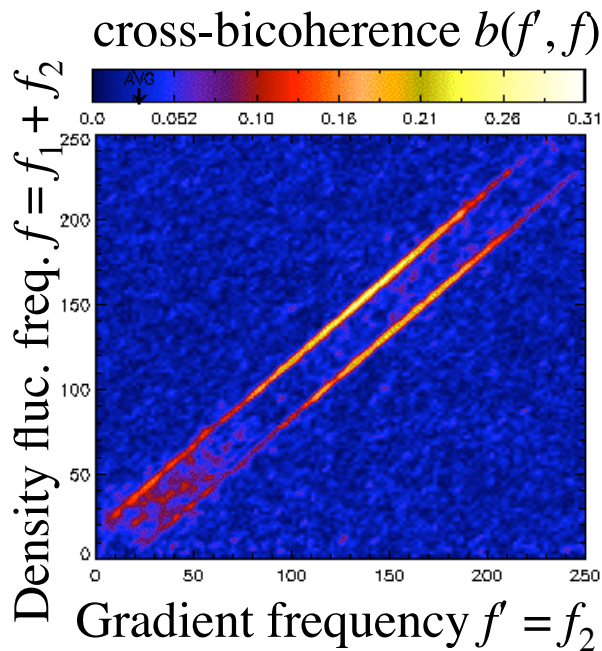
ω' (c_s/a)

Bicoherence in (f', f) vs. (f_1, f_2) Planes; Cross vs. Auto-Bicoherences

- Formulation in (f', f) and (f_1, f_2) planes equivalent ($f = f_3 = f_1 + f_2$, $f' = f_2$)

$$\frac{\langle \tilde{n}^*(f) V_y(f - f') \partial_y \tilde{n}(f') \rangle}{\sqrt{\langle |\tilde{n}(f)|^2 \rangle} \sqrt{\langle |V_y(f - f') \partial_y \tilde{n}(f')|^2 \rangle}} = b(f', f) \equiv b(f_1, f_2) = \frac{\langle \tilde{n}^*(f_1 + f_2) V_y(f_1) \partial_y \tilde{n}(f_2) \rangle}{\sqrt{\langle |\tilde{n}(f_1 + f_2)|^2 \rangle} \sqrt{\langle |V_y(f_1) \partial_y \tilde{n}(f_2)|^2 \rangle}}$$

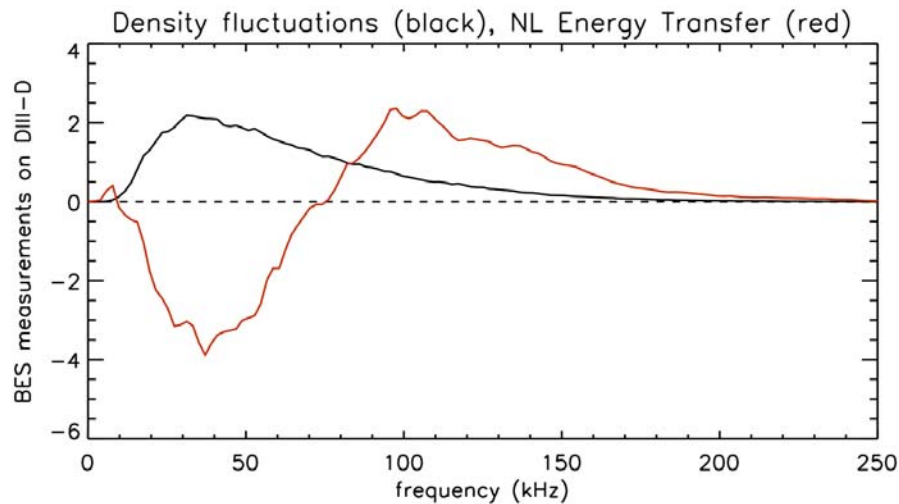
- Auto-bicoherence of BES signals (on right) both qualitatively and quantitatively different -> Illustrates danger in using "proxy" bispectra



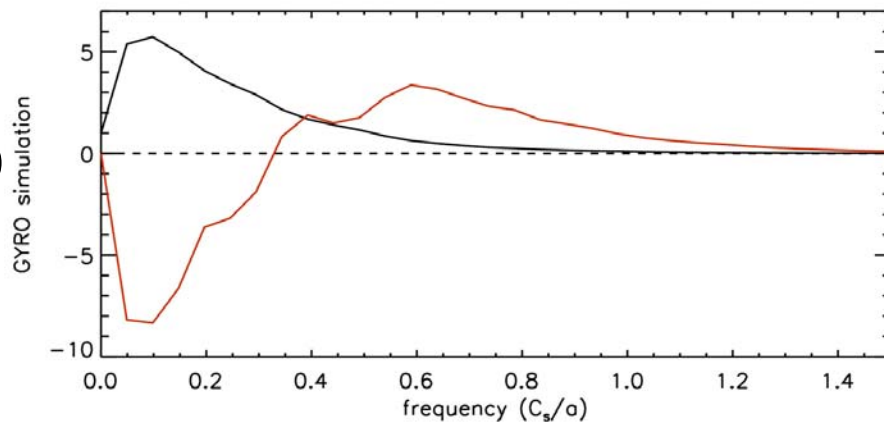
Integrated Transfer Functions Show Clear Similarities Between Experiment & Simulation, f and k -space

Frequency Space

DIII-D



GYRO



GYRO Wavenumber Space

